ARCHIVES
of
FOUNDRY ENGINEERING

ISSN (2299-2944)
Volume 2025
Issue 3/2025

213 – 220

10.24425/afe.2025.155370

24/3

Published quarterly as the organ of the Foundry Commission of the Polish Academy of Sciences

Computer Modeling of Layered Castings Solidification: Analysis and Optimization

A. Dulska *, N. Przyszlak
Silesian University of Technology, Faculty of Mechanical Engineering, Department of Foundry Engineering, Poland
* Corresponding author: E-mail address: agnieszka.dulska@polsl.pl

Received 25.07.2025; accepted in revised form 08.09.2025; available online 12.09.2025

Abstract

The aim of the article was to explore the principles of surface layer solidification based on computer simulations. The process was observed through computer simulations using the MAGMASOFT program. The studied model sets were separately parameterized in the system according to the conditions present during the casting process. Boundary conditions for FEM and technological data, such as pouring temperature and material, were defined. Based on the conducted studies, it was found that the solidification process of the layered casting, consisting of a base part made of cast iron and a working part made of pure titanium, is the most stable in the case of using an insert with the thinnest connector wall thickness (2.25 mm - these are the inner diameter of the profile) due to temperature equalization. However, this did not favor mechanical conditions compared to, for example, an insert with a medium connector wall thickness (1.5 mm - these are the inner diameter of the profile). The thickness of the connector wall influences the temperature distribution on the insert's surface and in its immediate area near the connection with the casting.

Keywords: Layered casting, Gray cast iron, Simulation

1. Introduction

Layered castings are used in various fields such as the automotive, aerospace, construction, and energy industries. They allow to create of structures and shapes aimed at enhancing the strength and mechanical properties of the cast components, thereby improving the quality and durability of the parts. This casting technology is frequently used due to the high functional properties provided by the surface layers of working parts that are exposed to wear. It is considered one of the most economical methods, as it enables the production of machine components with enhanced properties on selected surfaces directly during the casting process [1-6].

The properties of the surface layer of a casting primarily depend on the cooling and solidification conditions, as well as on the interaction between the metal and the mold surface - i.e., how the mold material affects the surface layer of the casting during pouring, solidification, and cooling.

Surface alloy layers formed directly in the process of pouring molten metal into specially prepared molds become particularly important for the casting's performance. This method increases the operational durability of cast components, especially those working in demanding service conditions, requiring high wear resistance and superior mechanical and ductile properties [7-15].

The technology of forming surface alloy layers on selected areas of a casting is used in industry to produce castings resistant to abrasive wear in dry friction conditions such as metal-to-metal or metal-to-mineral contact-for instance, with hard coal, lignite, or construction materials (gravel, sand, cement). The required properties of abrasion-resistant layers are achieved directly in the casting process by pouring steel or cast iron into sand molds equipped with alloy inserts placed on selected surfaces [1].

This technology requires proper preparation of the mold cavity with an alloying material (usually granular), in the form of a perforated insert 3–10 mm thick, bonded with an organic binder such as epoxy resin and organic solvent, or with water glass. Chromium carbide or silicon carbide powders with a grain size of 1.2–2.0 mm can also be used in the inserts, as well as nickel-based alloy powders with Ti (C, N) additives. Additionally, corundum with a grain size of 1.2–2.5 mm is used, along with Fe-Cr-C alloys as the base material with a grain size of 0.8–1.0 mm [2,3].

The primary alloying element in the surface layers formed on castings is chromium, with other elements such as manganese, boron, nickel, silicon, or vanadium. A key parameter is the grain size of the insert material. Layers made from finer-grain materials exhibit the best abrasion resistance.

Surface alloy layers are well characterized when the insert material contains alloying elements with significantly higher melting points than the poured metal, where the main process involves penetration of the molten metal into the porous surface layer of the material. However, the formation conditions of the surface alloy layer are not well-defined when the melting points of the insert material components are close to or lower than the temperature of the poured metal [5,6].

Nowadays, computer simulation of casting processes - i.e., virtual replication-plays an increasingly important role in the foundry industry. Simulation software is widely used by foundry engineers to facilitate and accelerate the design and manufacturing of new castings. These simulations allow prediction of molten metal behavior in the mold and enable observation of the physicochemical phenomena during metal solidification and cooling. Such programs provide significantly more information and process characteristics, making it easier and faster to identify and correct potential errors. Simulation software has become a fundamental tool in the ongoing efforts to improve casting quality [4].

In this study, the authors attempted to conduct model-based research on surface layers. The goal was to observe virtually the phenomena occurring inside a mold with an alloy insert during the pouring and solidification of the casting.

2. Methodology

The process of producing castings with a surface alloy layer is quite complex; however, there is a high demand in industry for castings that are wear-resistant while maintaining good ductility. The conducted research involved placing a preform in the mold cavity. During the pouring and filling of the mold, the elements from the insert diffuse into the casting, forming an alloy layer.

The study utilized a layered casting model consisting of two main structural components: a load-bearing part and a working element (insert). The working element was an insert made of pure titanium. In the real-world experiments, the insert was produced using 3D printing technology via the Selective Laser Melting (SLM) process, forming a spatial structure from powdered pure titanium.

To perform numerical simulation of solidification, the models of the base part and the insert were made using SolidWorks.

In the simulation studies, certain simplifications were adopted due to the nature of the software. The design of the insert consisted of rods with a circular cross-section and an outer diameter of 3 mm, intersecting symmetrically in both horizontal and vertical directions, spaced 7 mm apart (Fig. 1).

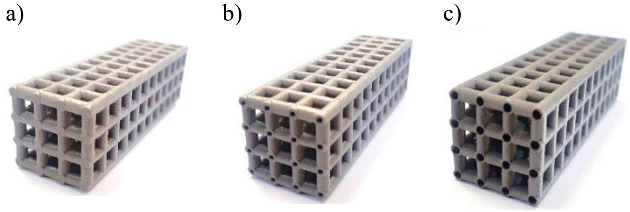

Fig. 1. Actual view of the insert – a) W0; b) W1.5; c) W2.25

The geometry of the insert varied in terms of the rod dimensions. The first variant featured a solid-fill geometry with an outer diameter of 3 mm and an inner diameter of 0 mm – W0 (Fig. 2a). The second had a hollow profile with an inner diameter of 1.5 mm – W1.5 (Fig. 2b), and the third also had a hollow profile with an inner diameter of 2.25 mm – W2.25 (Fig. 2c).

The simulation studies were conducted using the MAGMASOFT v.6.0 computer software, aimed at developing an experimental casting technology for alloy layers. The materials used in the simulation tests included an insert made of pure titanium and near-eutectic cast iron (EN-GJL-250), with a pouring temperature set at 1400°C.

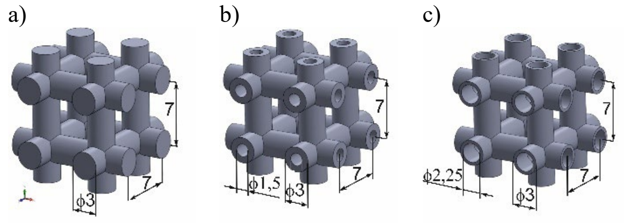

Fig. 2. Model of a single cell of the spatial insert – a) W0; b) W1.5; c) W2.25

As part of the study, a simulation of the solidification process was carried out. The virtual models of the castings are shown in Figures 3 and 4. In the first stage of the research, a simulation was performed for a single cell of the insert, maintaining all geometric parameters of the casting (Fig. 3). Subsequent studies involved the full dimensions of the model casting (Fig. 4).

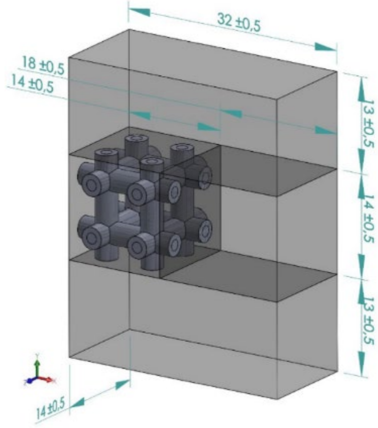

Fig. 3. Geometry of the virtual casting using a single insert cell

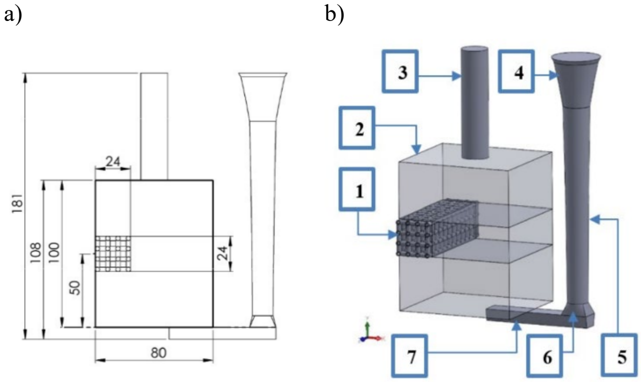

Fig. 4. Schematic of the model system of the layered casting; 1 – spatial titanium insert, 2 – cast iron casting, 3 – overflow, 4 – pouring basin, 5 – main sprue, 6 – runner, 7 – ingate

To carry out the computer simulation, it was necessary to define the thermophysical properties of the materials used (data from the MAGMASOFT database) for cast iron, titanium, and furan sand (used for the mold). In addition to thermophysical properties, the initial parameters of the individual materials had to be taken into account:

- Insert temperature – 20°C
- Mold temperature – 20°C
- Ambient temperature – 20°C
- Molten metal temperature – 1400°C
- Pouring time – 5 s
- Linear speed of metal rising in the mold – 3 cm/s
- Mesh parametres: presented in Table 1.

Table 1.
Mesh parameter values applied to individual parts of the given casting

Casting designation	Gray cast iron casting	Furan mold	Mold cavity in the insert between the connectors	insert	Cast iron-filled space in the connector of the insert	Number of cartesian cavity cells
	mm					
For the variant presented in Fig. 5						
W0	5	5	0,5	0,5	-	321 600
W1,5	5	5	0,5	0,37	0,37	554 788
W2,25	5	5	0,5	0,38	0,38	646 328
For the variant presented in Fig. 8						
W0	5	5	1,5	1,5	-	641 131
W1,5	5	5	3	0,8	0,8	613 768
W2,25	5	5	3,5	0,626	0,8	650 763

3. Discussion of the results

The computer simulation of the solidification process of the layered casting was performed using the MAGMASOFT v. 6.0. The layered casting was obtained in a solid–liquid system. The aim of the study was to observe the processes occurring inside the mold, the temperature distribution within the insert, and in the space between the individual elements of the insert. The analyzed system is not without flaws, mainly due to certain simplifications inherent to the software's capabilities. The results of the temperature distribution simulation for the scaled-down casting are shown in the following figures (Fig. 5). They show the temperature distribution for three different inserts, recorded at three different times after the mold was filled.

The outcome of the conducted computer simulations also included a set of temperature vs. time curves (Fig. 6) for individual measurement points. The measurement locations—i.e., the placement of thermocouples—are shown in Figure 7. The maximum temperatures recorded at these points are presented in Table 2.

Table 2.
Maximum temperature values for individual measurement points from thermocouples placed in the scaled-down inserts (T – Thermoelement)

Insert	T1	T2	T3	T4
	ºC			
W0	1400	1148	1147	1400
W1.5	945	947	947	958
W2.25	1399	946	951	959

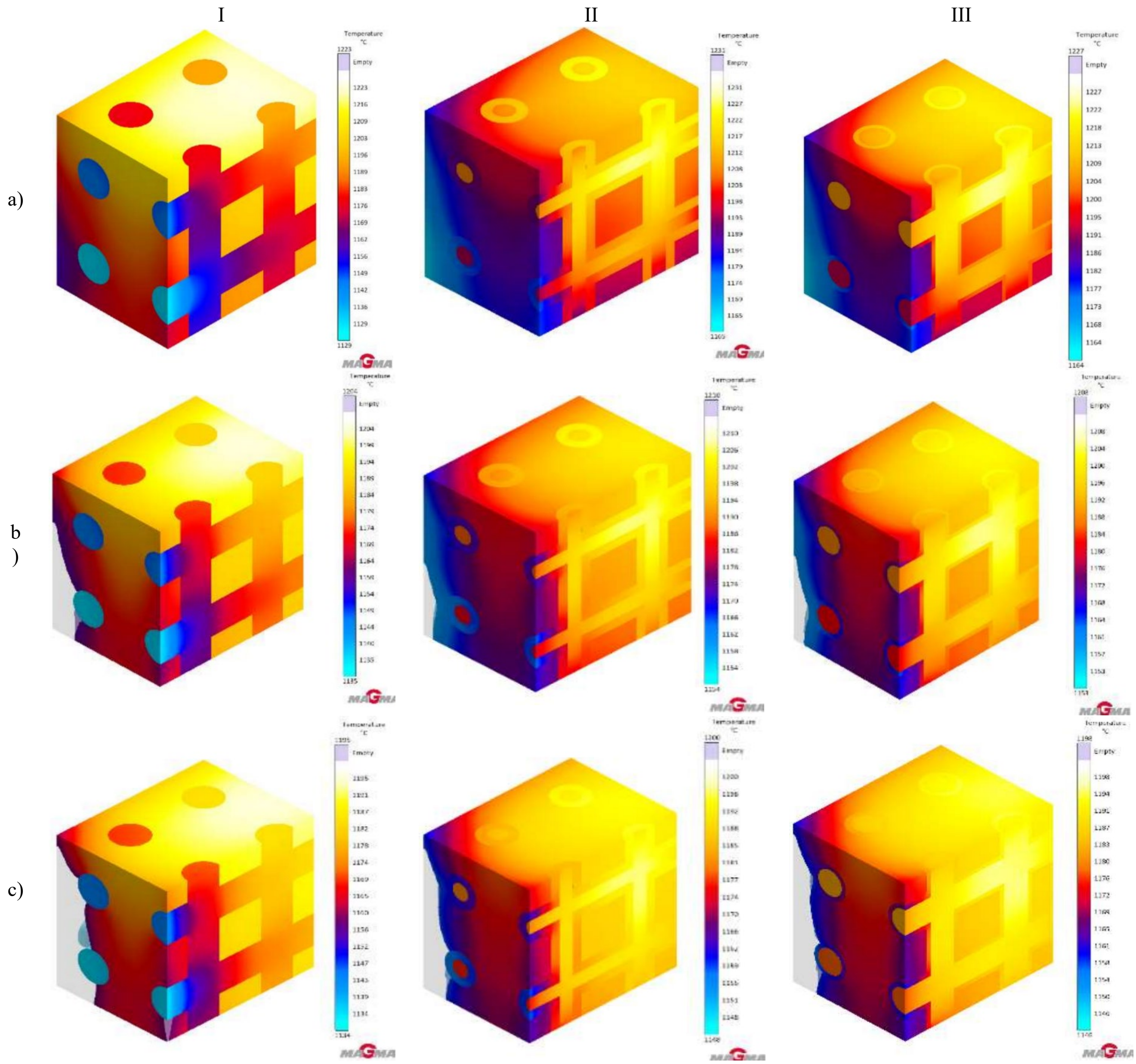

Fig. 5. Results of the computer simulation of temperature distribution for inserts I – W0; II – W1.5; III – W2.25: a) temperature distribution after 14 seconds of pouring; b) temperature distribution after 17 seconds of pouring; c) temperature distribution after 18 seconds of pouring

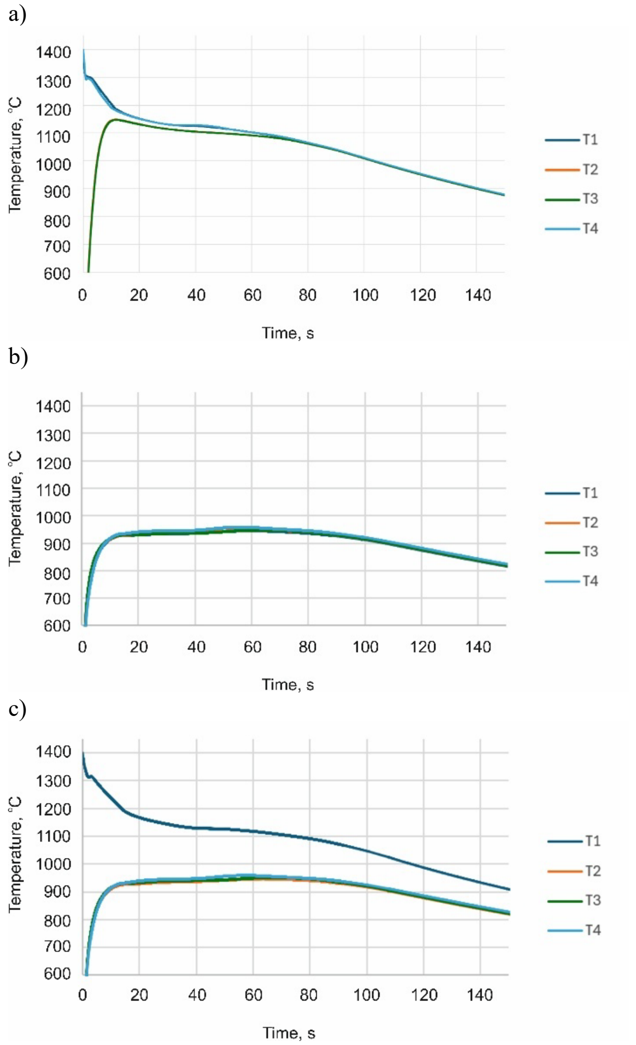

Fig. 6. Temperature distribution graphs over time for the applied scaled-down inserts: a) W0; b) W1.5; c) W2.25

Comparing the temperature distribution between castings with inserts W0, W1.5, and W2.25 (Fig. 5a) after 14 seconds of pouring, we can observe that in the W0 insert (solid fill), the highest temperature occurs in the central-inner part of the casting insert, approximately 1230°C. The temperature distribution in this area is influenced by the flowing molten metal. The temperature of the W1.5 insert, considering the same pouring time, differs slightly due to its lower heat capacity; the temperature in the central part is lower than in W0, about 1200°C. The front zone of the casting already has a lower temperature caused by the cooling of the casting. Meanwhile, the internal fill of the insert cell in the upper part of the casting maintains the highest temperature, around 1230°C. It can be assumed that the molten metal that entered the inner channel of the titanium insert cell solidifies more slowly, but the casting loses heat faster to the outside. Considering the W2.25 insert, the highest temperature was recorded in the inner cell area (cast iron) and in the titanium insert wall layer.

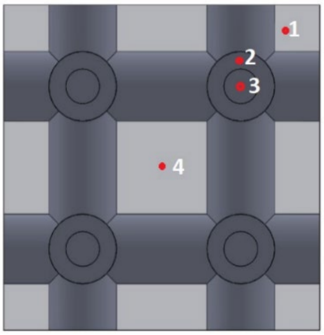

Fig. 7. Placement of thermocouples in the casting: Thermocouple 1 – at the junction near the insert wall and casting, Thermocouple 2 – in the area of the inner cell of the insert wall, Thermocouple 3 – in the area of the central-inner cell of the insert, Thermocouple 4 – cast iron casting in the insert connector

Observation and comparison at the second time interval, 17 seconds, show a very similar situation with a slight temperature drop throughout the entire casting for all three types of inserts, especially in the outermost areas of the insert and the walls at the external corners of the casting and the cells.

The temperature distribution conditions at 18 seconds are as follows. The highest temperature, around 1180°C, is present in the upper part of the W0 insert (Fig. 5c). The gravitational heat generated during pouring and the final settling show that heat is first released outward from the corner zones and areas adjacent to the insert, especially the solid one. In the W1.5 insert (Fig. 5c), the colors blue, dark blue, and violet indicate that the solidification structure changes more rapidly around the insert cells. In the W2.25 insert (Fig. 5c), the internal fill of the cell demonstrates and confirms that the molten metal inside the cells releases heat more slowly.

The second stage of the study concerned simulation tests for castings with a full-size insert (Fig. 4). The models were parameterized in the same way as for the scaled-down insert. The only difference was the mesh size for the individual parts of the casting, mainly due to the computational capacity of the research workstation. Figures 8 and 9, as well as Table 3, show the temperature distribution at the measurement points for the applied insert.

Analyzing the temperature distribution for the full-size W0 insert (solid fill) from Fig. 8, we can observe that part of the insert has the lowest temperature, around 20°C, on the outer side of the casting. After 3 seconds of pouring, the upper part of the insert profile becomes covered, marking the beginning of gradual heating and filling of the casting volume. In Fig. 8, it becomes evident how the metal stream is directed straight toward the insert profile, progressively transferring temperature layers to the outside.

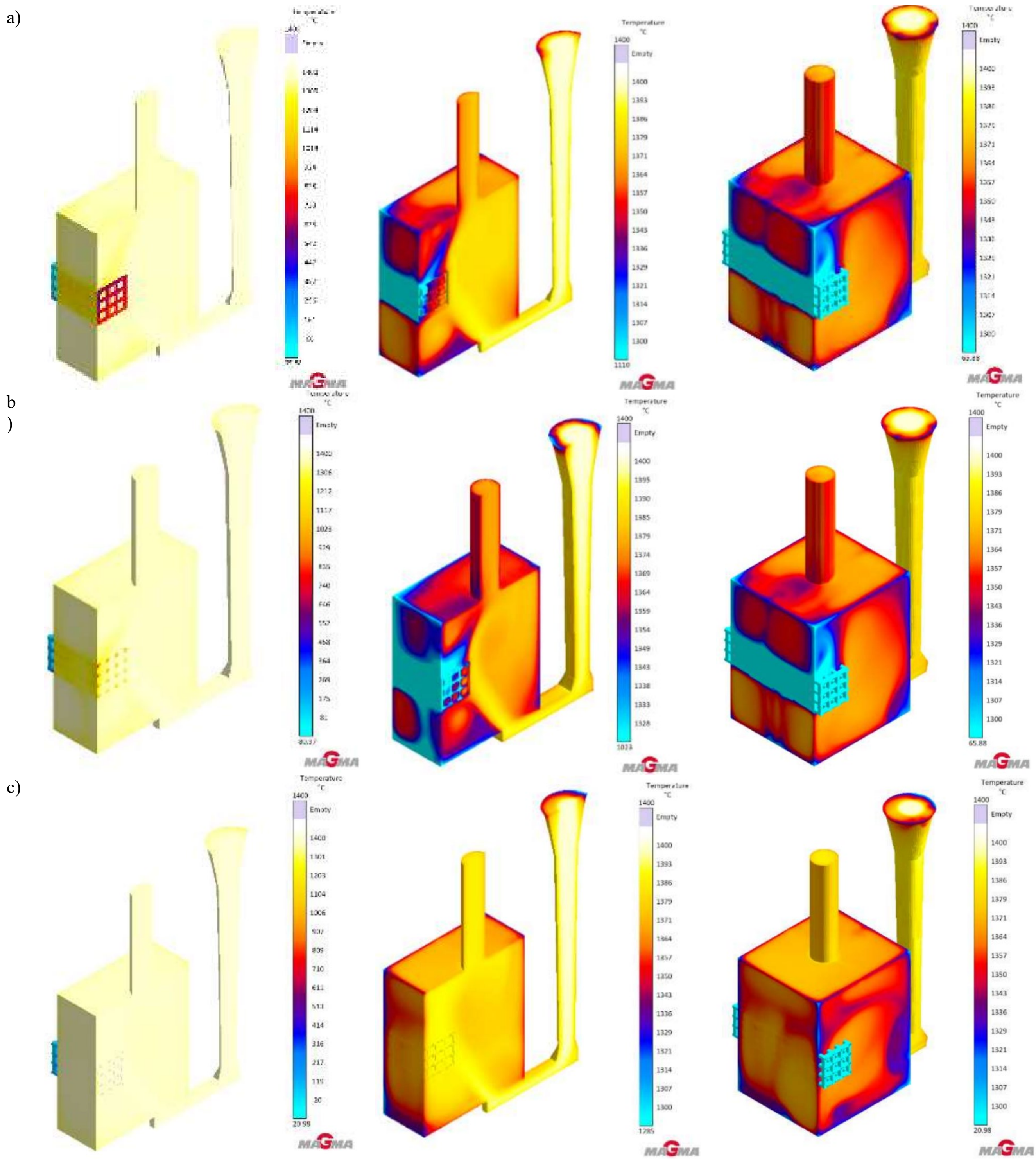

Fig. 8. Temperature distribution in the casting during pouring for the full-size insert after 5 seconds: a) W0; b) W1.5; c) W2.25

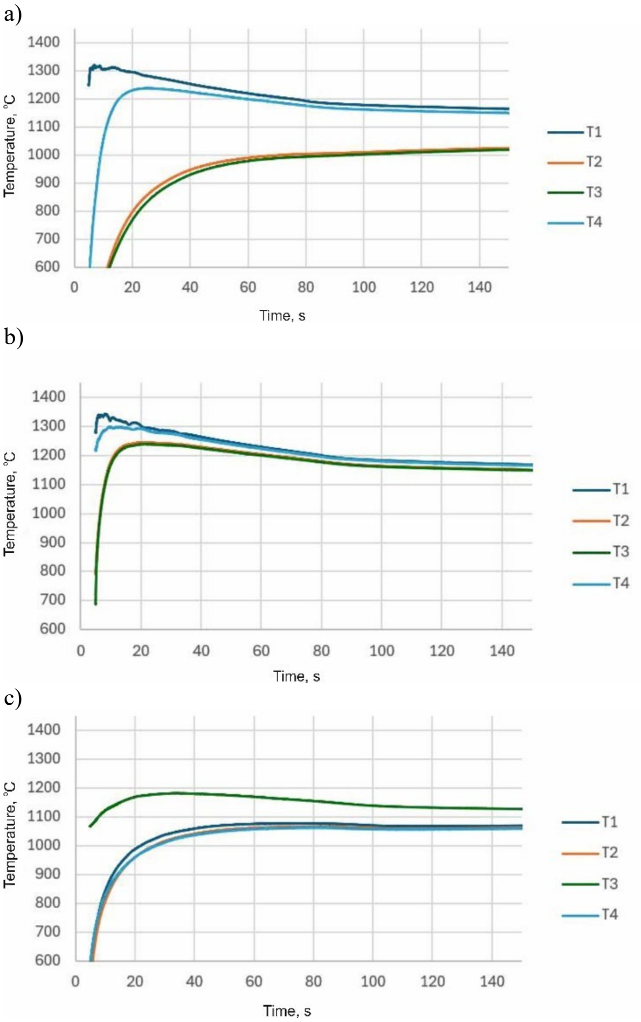

Fig. 9. Temperature distribution graphs over time for the applied full-size inserts: a) W0; b) W1.5; c) W2.25

Table 3.
Maximum temperature values for individual measurement points from thermocouples placed in the full-size inserts
(T – Thermoelement)

Insert	T1	T2	T3	T4
	ºC			
W0	1319	1053	1049	1237
W1.5	1341	1245	1238	1297
W2.25	1077	1073	1181	1072

Describing the W1.5 insert (Fig. 8c), we can see that the temperature and cooling direction shift to the upper part of the casting, i.e., from the part of the insert protruding upwards. It can be inferred that this temperature distribution acts as a natural cooling factor for the casting part extending beyond its volume, functioning somewhat like a heat sink.

The last insert considered in terms of temperature distribution is the W2.25 insert. Due to its profile (with thin walls), heat penetrates through the structure very quickly, resulting in a temperature of about 1380°C. After 4 seconds, the temperature distribution was almost uniform, ranging from 1350 to 1390°C. At 5 seconds, a temperature drop in the corner zones to approximately 1330°C was observed. Meanwhile, the temperature in the internal zone of the insert equalized with the casting temperature, which suggests that molten metal diffused through the casting walls due to the diameter.

4. Conclusions

In summary, based on the course of the research and the results obtained, it can be concluded that the solidification process of the layered casting-consisting of a cast iron supporting part and a pure titanium working part-showed that the most stable process occurred in the W2,25 insert due to temperature equalization; however, this did not positively affect the mechanical conditions compared to, for example, the W1,5 insert. The thickness of the connector wall influences the temperature distribution on the surface of the insert as well as in its immediate vicinity at the boundary with the casting. A very important factor affecting the course of the computer simulation is the proper definition of boundary conditions and the appropriate division of mesh nodes in the finite element mesh (FEM) for each area of the studied object.

References

[1] Wróbel, T. (2016). *Layered castings made by preparing the mold cavity with a monolithic insert*. Gliwice: Wydawnictwo Archives of Foundry Engineering, Monografia. (in Polish).

[2] Przyszlak, N., Wróbel, T. & Dulska A. (2021). Influence of molding materials on the self-hardening of X46Cr13 steel / grey cast iron bimetallic castings. *Archives of Metallurgy and Materials*. 66(1), 43-50. DOI:10.24425/amm.2021.134757.

[3] Przyszlak, N., Wróbel, T., Dulska, A., Nuckowski, P., Łukowiec, D. & Stawarz, M. (2024). Microstructure of the working layer of X46Cr13 steel in a bimetal system with gray cast iron. *Materials.* 17(23), 5933, 1-13. https://doi.org/10.3390/ma17235933.

[4] Przyszlak, N. & Piwowarski, G. (2023). Designing of X46Cr13 steel heat treatment in condition of casting mould. *Archives of Foundry Engineering.* 23(2), 119-126. DOI: 10.24425/afe.2023.144304.

[5] Gawroński, J., Szajnar, J., Cholewa, M. & Wróbel, P. (2005). Solidification and crystallization of the particles containing composites and surface composites. *Przegląd Odlewnictwa*. 55(4), 216-230. (in Polish).

[6] Gawroński, J., Szajnar, J. & Wróbel, P. (2006). Technology of surface composite layers on castings. *Archiwum Odlewnictwa.* 6(19).

[7] Fathy, N., Ramadan, M., Hafez, K.M., Abdulaziz, B.A, Ayadi, B. & Alghamdi, S.A. (2023). A novel approach of optimum time interval estimation for Al-7.5Si/Al-18Si liquid–liquid bimetal casting in sand and metallic moulds. *Materials*. 16(8), 3004, 1-11. DOI: 10.3390/ma16083004.

[8] Nazari, J., Yousefi, M., Amiri Kerahroodi, M.S Bahrololoumi Mofrad, N.S. & Alavi Abhari, S.H. (2015). Production of

copper-aluminum bimetal by using centrifugal casting and evaluation of metal interface. *International Journal of Materials Lifetime*. 1(1), 20-28. DOI:10.12691/ijml-1-1-4.

[9] Łągiewka, M. (2019). Determination of thermophysical properties for selected molding sands. *Acta Physica Polonica A*. 136(6), 992-995. DOI: 10.12693/APhysPolA.136.992.

[10] Wróbel, T. & Szajnar, J. (2015). Bimetallic casting: ferritic stainless steel-grey cast iron. *Archives of Metallurgy and Materials*. 60(3), 2361-2365. https://doi.org/10.1515/amm-2015-0385.

[11] Król, M. & Tański, T. (2016). Surface quality research for selective laser melting of Ti-6Al-4 V alloy. *Archives of Metallurgy and Materials*. 61(3), 1291-1296. https://doi.org/10.1515/amm-2016-0213.

[12] Yesuvadian, R.A. & Keerthiprasad, K.S. (2023). A review on casting and testing of bimetals. *International Journal of Applied Engineering Research.* 18(4), 278-291. https://dx.doi.org/10.37622/IJAER/18.4.2023.278-291.

[13] Xiong B., Cai, C., Wan, H. & Lu, B. (2011). Fabrication of high chromium cast iron and medium carbon bimetal by liquid- solid casting in electromagnetic induction field. *Materials and Design*. 32(5), 2978-2982. https://doi.org/10.1016/j.matdes.2011.01.006.

[14] Ibrahim, M.M., El-Hadad, S. & Mourad, M. (2020). Effect of liquid-solid volume ratios on the interfacial microstructure and mechanical properties of high chromium cast iron and low carbon steel bimetal. *Material Researches Express*. 6(12), 1265c2, 1-12. DOI 10.1088/2053-1591/ab6372.

[15] Wei, N., Wang, K., Zhou, X., Wang, Q., Liu, Q. & He, J. (2012). Influence of cooling rate on the microstructure in HCCI/steel bimetal composite hammer. *Advanced Materials Research*. 538-541, 1041-1044. https://doi.org/10.4028/www.scientific.net/AMR.538-541.1041.